

## Numerical simulation the bottom structures grounding test by LS-DYNA

Ainian Zhang

Graduate School of Frontier Sciences, The University of Tokyo,  
7-3-1 Hongo Bunkyo-ku, Tokyo, JAPAN, 113-8656

Katsuyuki Suzuki

Graduate School of Frontier Sciences, The University of Tokyo,  
7-3-1 Hongo Bunkyo-ku, Tokyo, JAPAN, 113-8656

**Keywords:**

Nonlinear FEM, Grounding test, Numerical simulation, Parameters analysis

**Abstract**

Nonlinear finite element method (FEM) is a powerful tool for analyzing ship collision and grounding problems. The reliability of the numerical simulation results largely depends on the proper definition of problem and careful control of some critical parameters. The purpose of the paper is to study the effect of selected parameters on crashworthiness of the single-hull bottom structure due to raking. The quasi-static grounding process is simulated by the LS-DYNA code. The effects of the following parameters are considered: the boundary condition, the friction coefficient, shell element type, the residual stress and the material model. The influences of selected parameters are assessed by comparing the different results in the impact force and absorbed energy vs. penetration of rock model. Some suggestions are proposed for numerical simulation in finite element code LS-DYNA.

## 1 Introduction

Most papers considering ship collisions and grounding using finite elements have been published within the last decade. The modeling of the structure is quite laborious to set up and the simulation requires considerable hardware resources to perform. However, as computer technology progresses it becomes relatively easier to simulate impacts on large and complicated structures. Today it is possible to simulate collisions and grounding involving large ship structures with thousands of degrees of freedom even at the PC level. Many powerful FEM codes that have been used for the simulation of ship collision and grounding are the explicit DYTRAN, RADIOSS, ABAQUS/Explicit, LS/DYNA3D, and the implicit NASTRAN, ABAQUS/Standard, ANSYS, MARC.

One of the pioneering studies involving finite-element simulations has been performed by Vredevedt et al (1993). Those numerical simulations have considered the collision adequacy of inland vessels using MSC/Dytran. Some recent literature on numerical simulations of collision and grounding include Mizukami et al (1996), Kuroiwa (1996), Kitamura (1998, 2001), Servis & Samuelides (2000), Endo (2001), Wu et al. (2004).

Nonlinear finite element method (FEM) is a powerful tool for analyzing ship collision and grounding problems. The reliability of the numerical simulation results largely depends on the proper definition of problem and careful control of some critical parameters in FEM code. Servis et al (2002) attempted to determine the parameters that largely influence ship collisions in finite element code. Krzysztof (2003) studied the effect of parameters on crashworthiness of the struck ship by ABAQUS/Explicit code. The purpose of the paper is to study the effect of selected parameters on crashworthiness of the single-hull bottom structure due to raking. The effect of the following parameters are considered: the boundary condition, the material model of the bottom structures, different shell element types, the friction coefficient for the contact between the bottom structures and the rock, the residual stress of the bottom structures.

## 2 Bottom structures grounding experiment

In 1993, Association for Structural Improvement of the Shipbuilding Industry (ASIS) carried out the static failure experiments of bottom structures due to bottom raking to examine characteristics of the structural failure of oil tanker. Fig. 1 shows a schematic view of the experiments.

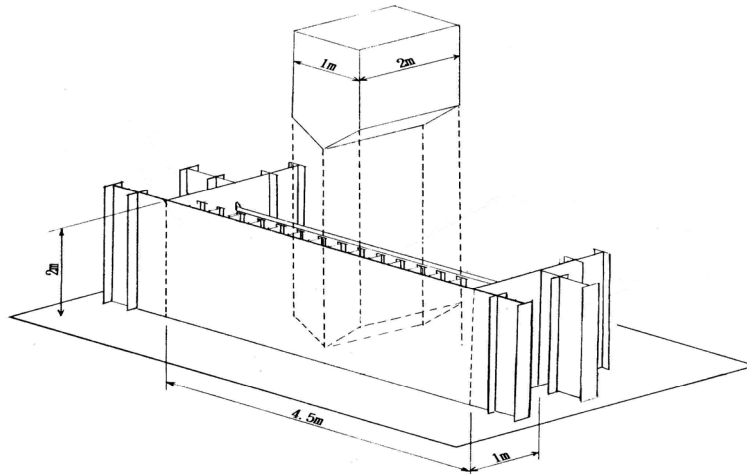


Fig.1 Schematic view of the experiment

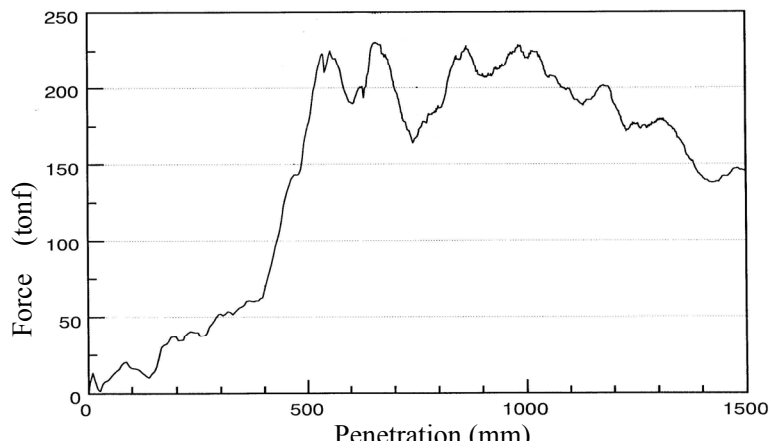


Fig.2 Relationship between penetration and force

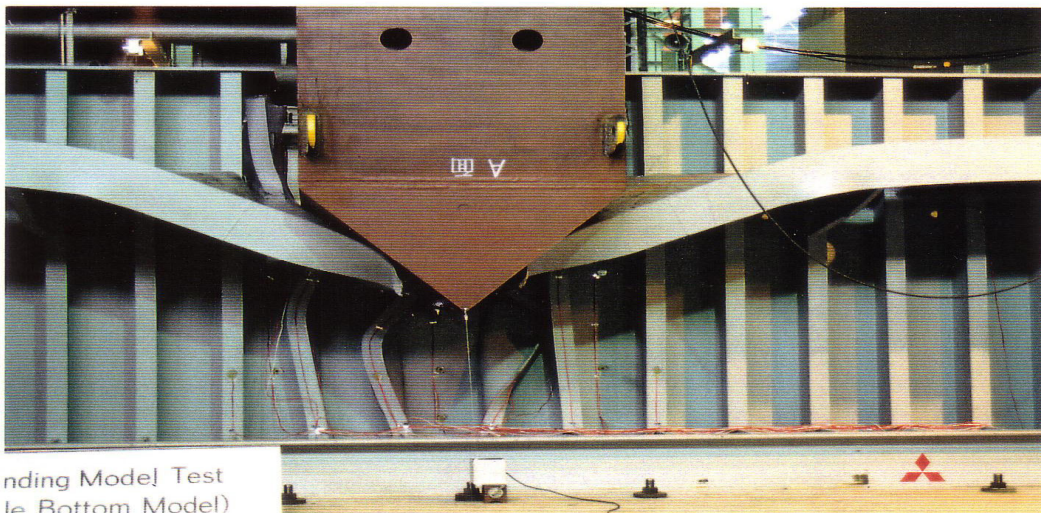


Fig.3 Deformation and failure during experiment

A wedge-shaped rigid rock model which was fixed to a press machine was pushed against the bottom model along the direction of ship length quasi-statically. The single-hull bottom model with 1/3 scale of a VLCC

bottom structure was tested. The model was made of steel plate, of which the yield stress was 323MPa on average. The relationship between raking force and penetration length of the single-hull model is shown in Fig. 2. Fig. 3 shows one picture taken during the experiment.

### 3 Numerical model

The general purpose finite element program LS-DYNA was used to recreate the experiment through numerical simulation. Data pre/post-processing was done by Jvision.

The single-hull bottom model is modeled as thin shell element. The wedge-shaped rigid rock model is modeled as rigid body. Fig. 4 shows the meshed model of bottom structures.

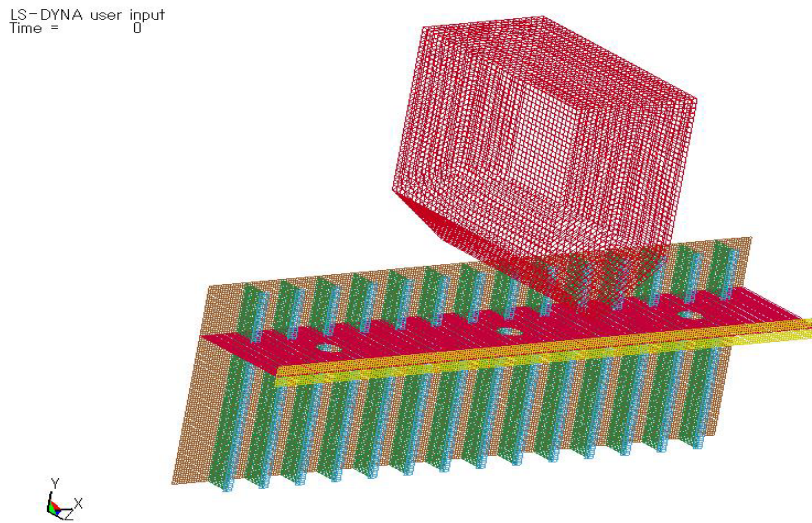


Fig.4 The meshed model of bottom structures

The wedge-shaped rigid rock model was slowly pushed into bottom structures at a speed of 0.93mm/s to reflect the quasi-static test condition. Through monitoring dynamic energy and ensuring that the majority of impact energy was dissipated in the deformed structures, attention in calculation was paid to the selection of rock model speed to achieve a reasonable balance between calculation accuracy and cost (CPU time). In the numerical simulation, the moving speed of rock model was given to be 6.0m/s.

Since the physical boundary condition was not explicitly modeled in the numerical simulation, two types of the boundary conditions were applied at the edge of bottom structures. This aspect will be discussed further in the next section of this paper

The contact between the bottom model and the rock model and the contact between each part of the bottom structures were considered. The actual friction coefficient associated with the contacts was difficult to assess, therefore a parametric study for friction coefficient was performed. This aspect will also be discussed further in the next section of this paper

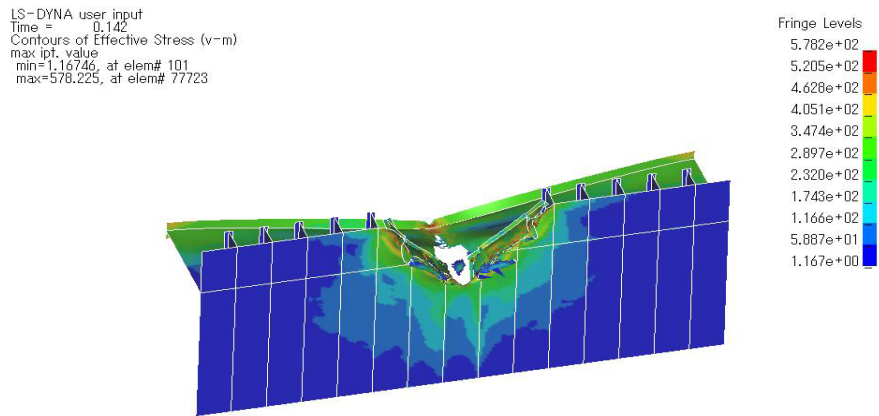


Fig.5 Deformation and failure by numerical

Material failure was considered in the model using strain failure criterion. If the calculated effective plastic strain for any element exceeds the predefined value, the element will be removed from the model and the simulation continues with the eroded model.

Fig. 5 shows the numerical simulation of deformation and failure of bottom structure. The impact force and absorbed energy curves are presented in Fig. 6

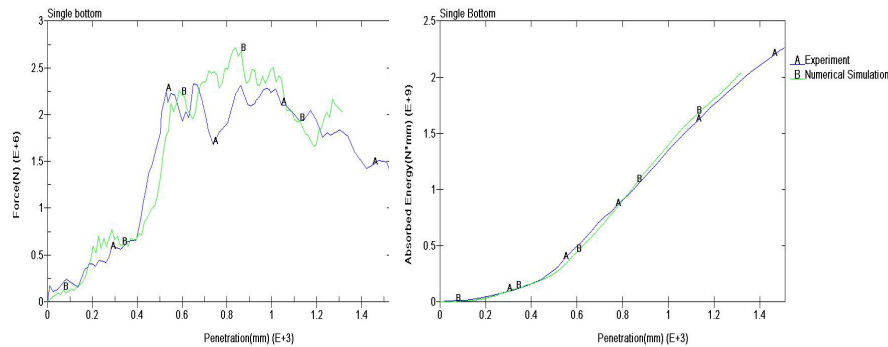


Fig.6 Impact Force and absorbed

#### 4 Influence of selected parameters of analysis

The effects of selected parameters are measured by comparing the different results in the impact force and absorbed energy vs. penetration of rock model, such as the material model of the bottom structures, different shell element types, the friction coefficient for the contact between the bottom structures and the rock, the residual stress of the bottom structures.

##### 4.1 Boundary condition

Since the physical boundary condition is not explicitly modeled in the numerical simulation, two types of the boundary conditions are applied at the edge of bottom structures:

- BC1 All displacements and rotations were suppressed
- BC2 All displacements were suppressed

To study the effect of boundary condition, the same values of the other parameters are used.

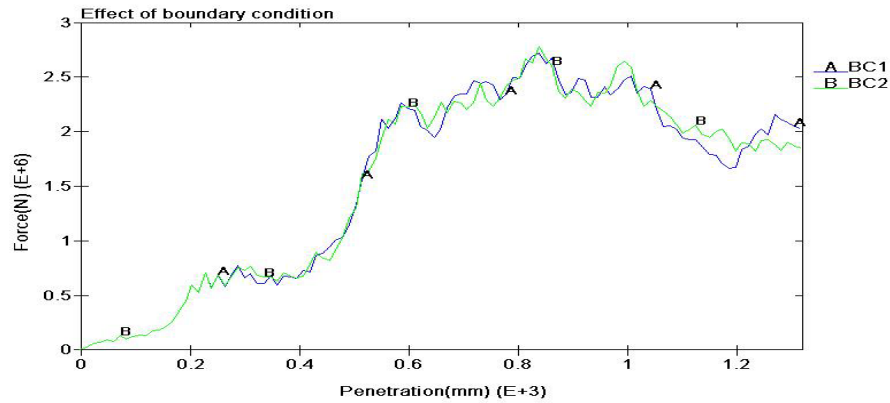


Fig.7 Penetration-impact force curve for different boundary conditions

Fig.7 shows the force-penetration curves for different boundary conditions BC1 and BC2. We can see that the difference between the force-penetration curves for BC1 and BC2 is much smaller. There is an error of 1.8% in the maximum impact forces between BC1 and BC2. The obtained results indicated that the impact force is insensitive to the boundary condition type. We suppose that the supports for the bottom structures in the experiments were rigid enough. In the following numerical model, all displacements and rotations at the edge of bottom structures were restricted.

#### 4.2 Friction coefficient

In numerical simulation, contact between the bottom model and the rock model and contact between each part of the bottom structures need to be considered. However the actual friction coefficient associated with the contacts is difficult to assess. According to LS-DYNA user manual, under normal dry surface condition, the friction coefficient on mild-steel-on-mild-steel surface is 0.74 for static friction and 0.57 for sliding friction. In engineering practice, both the static and dynamic friction coefficients equal 0.3 are used in most case and the value of friction coefficient larger than 0.6 is rarely used. Therefore it is necessary to perform a parametric study for friction coefficient. The values of friction coefficient equal 0.0, 0.2, 0.3, 0.4 and 0.55 are applied for parametric study. To study the effect of friction coefficient, the same values of the other parameters were used.

Fig. 8 shows that the impact force increases as the friction coefficient increases. In comparison with the case without friction, the impact force significantly increases when the friction coefficient equal 0.55 is applied. The maximum impact force increases approximately 60% while the friction coefficient increases from 0 to 0.55. We can also see that the difference between the curves for 0.3 and 0.55 is much less than the difference between the curves for 0.0 and 0.2.

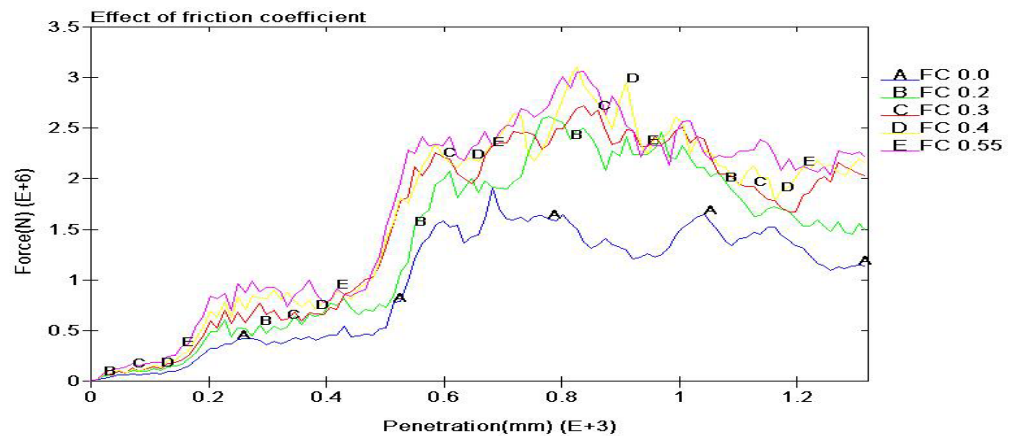


Fig.8 Penetration-force curve for different friction coefficients

The friction coefficient has significant influence on the history of impact force when it is in the range from 0 to 0.3. The impact force becomes insensitive to the friction coefficient when it increases from 0.3 to 0.55. We can expect that the effect of the friction coefficient on impact force will not become remarkable when the value of friction coefficient larger than 0.55.

#### 4.3 Shell element type

There are different kinds of shell elements available in LS-DYNA for modeling ship structures in order to perform nonlinear impact analyses. Belytschko-Tsay (BT) shell element as a computationally efficient has become the default shell element formulation in LS-DYNA. Since BT shell element is based on a perfectly flat geometry, warpage is not considered. The effect of neglecting warpage in bottom model grounding experiment cannot be predicted beforehand and may lead to less than accurate results, but the latter is difficult to verify in practice. Belytschko-Wong-Chiang (BWC) shell element can consider the warping stiffness with reasonable added computational cost.

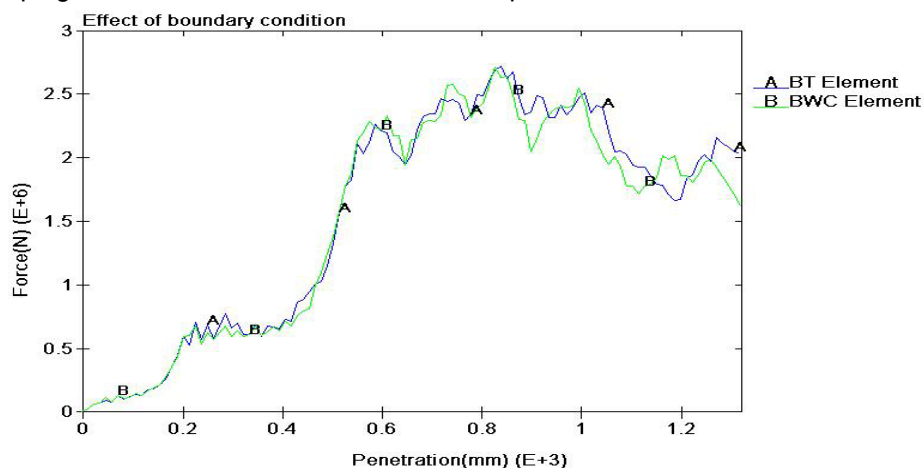


Fig.9 Penetration-force curve for different element types

Belytschko-Tsay shell element and Belytschko-Wong-Chiang shell element are applied in numerical simulation respectively. The effect of shell element type on penetration-force curve is shown in Fig. 9. The obtained



results indicate that the difference of penetration-impact force curves between BT shell element and BWC shell element is much smaller. However the calculation time increases approximately 40% using BWC shell element instead of BT shell element. If adequate mesh size is applied, good predicted result can be obtained for nonlinear impact analysis using BT shell element.

#### 4.4 The residual stress

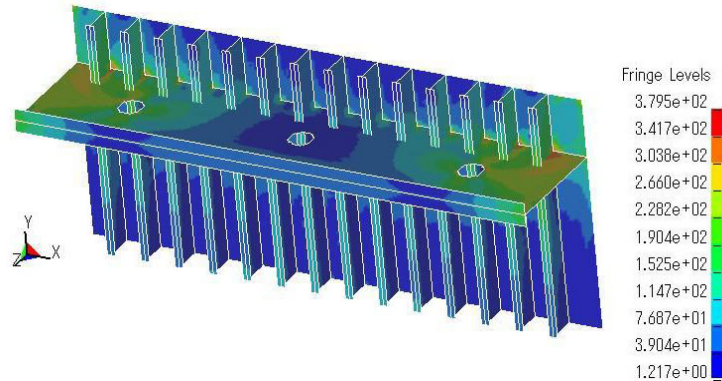


Fig.10 Residual stress due to initial imperfection

Since geometric imperfections and welding in the bottom structures will induce the residual stress, the effect of residual stress on the impact force is conducted. The residual stress had been calculated by moving the upper edge nodes of bottom structure about 5mm displacement in horizontal direction while the nodes of other three ends are restricted. The residual stress of the bottom structure is shown in Fig. 10. In this exercise, the residual stress caused by initial geometric imperfections is considered simply. Then FE analysis is conducted using pre-estimated residual stress as the initial stress. Histories of impact force and absorbed energy is shown in Fig. 11 as well as the result of without residual stress. The difference between two curves is much small. In this case, the maximum impact force has increased 10.6% when the residual stress is applied. Kitamura (2001) performed several large-scale finite element simulations of ship-ship collisions coupling ship collision and horizontal hull girder bending. He showed that effect of the horizontal hull girder bending could lead to less energy absorption capability and also earlier collapse of the ship structure. The influence of residual stress on the structural crashworthiness should be studied in future.

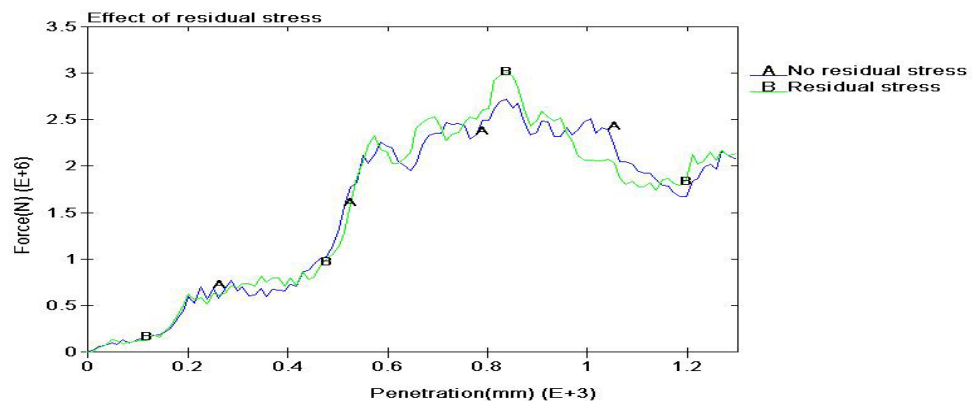


Fig.11 Penetration-force curve due to residual stress

## 4.5 Material model

Since the bottom structure grounding experiment involves extreme structural behaviour with both geometrical and material nonlinear effects, the input of material properties up to the ultimate tensile stress has a significant influence on the extent of absorbed energy of bottom structure. It is noted that the true stress-strain characteristics of the material are required in the non-linear finite element code LS-DYNA. The true stress and strain are related to engineering (or nominal) stress and strain as follows:

$$\sigma_{true} = \sigma_{eng} (1 + \varepsilon_{eng}), \quad \varepsilon_{true} = \ln(1 + \varepsilon_{eng}) \quad (1)$$

In most case, only limited material properties are available on the test setup, which are shown in Table 1. In generally, the material model is defined as an elastic-perfectly plastic material model (Mat.1). The true stress-strain curve based on the ultimate stress and the failure strain (Zhang 2004) is given in the following way (Mat.2).

$$\sigma = C \cdot \varepsilon^n \quad (2)$$

$$n = \ln(1 + \varepsilon_f) \quad (3)$$

$$C = \sigma_u \left( \frac{e}{n} \right)^n \quad (4)$$

Where  $\varepsilon_f$  is the failure strain;  $\sigma_u$  is the ultimate stress;  $e$  is the natural logarithmic constant.

Table 1 Material property of 4.5mm thickness plate

Yield Strength (MPa)	Ultimate strength (MPa)	Rupture strain	Young's Modulus (MPa)	Poisson Ratio
329.28	448.78	0.35	205800	0.3

If the tensile coupon tests of plates were conducted, the stress-strain curve obtained from the experiment can be used in numerical simulation (Mat.3). Three types of true stress-plastic strain curves of 4.5mm plate are shown in Fig. 12.

The effect of material types on the histories of impact force and absorbed energy is shown in Fig. 13. Since both the strain-hardening and necking effects are not taken into account in material model 1, it results in lower impact force and lower energy absorption capacity. Numerical results of material model 2 and 3 have the same penetration-absorbed energy curves. In numerical simulation, if only limited material properties are available, the material model 2 is recommended and good prediction of impact force and absorbed energy curve can be obtained.

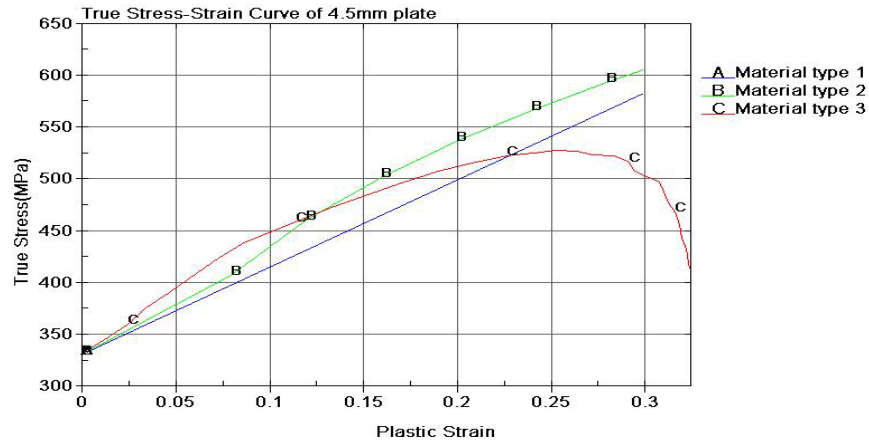


Fig.12 True stress-plastic strain curves for three types of material model

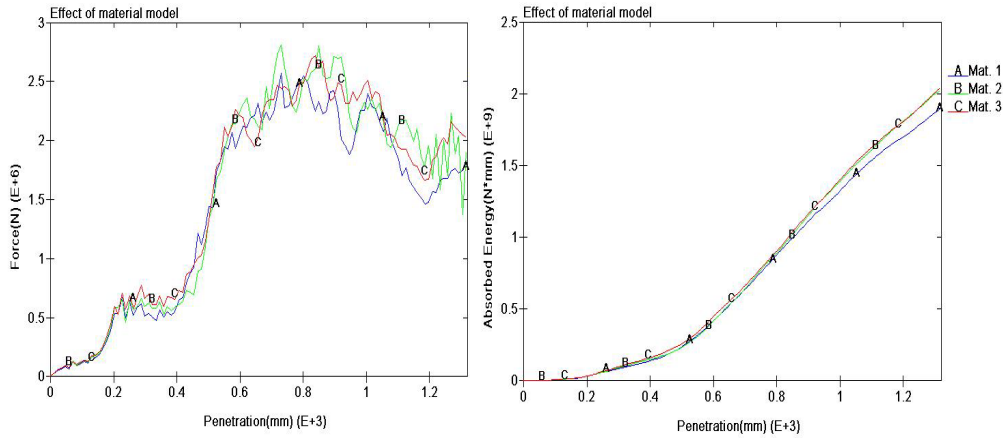


Fig.13 Impact force and absorbed energy

## 5 Conclusion

In this paper, the effect of selected parameters on crashworthiness of the single-hull bottom structure due to raking was studied. In computer simulations, the effect of boundary condition on the structural crashworthiness is small. When the value of friction coefficient is in the range from 0 to 0.3, it has significant influence on the history of impact force. Its influence becomes insensitive when the value of friction coefficient is more than 0.3. FE model using Belytschko-Tsay shell element can give good predicted result for nonlinear impact analysis if adequate mesh size is applied as well as low CPU time. Both material model 2 and 3 can give good numerical simulation. If only limited material properties are available, the material model 2 is recommended. In this case, FE model with residual stress can increase the value of the maximum impact force. The effect of residual stress should be studied in detail in future.

## 6 Acknowledgements

The author would like to thank Association for Structural Improvement of the Shipbuilding Industry (ASIS) for providing the experimental data.

**References**

Endo, H., and Yamada, Y., 2001. The Performance of Buffer Bow Structures against Collision (1st Report: Collapse Strength of the Simplified Structure Models). Journal of the Society of Naval Architects of Japan, Vol. 189, 209-217.

Kitamura O., 2001. FEM approach to the simulation of collision and grounding damage. The second International Conference on Collision and Grounding of ships. Copenhagen, Denmark, July 1-3.

Kitamura, O., Kuroiwa, T., Kawamoto, Y. and Kaneko, E., 1998. A Study on the Improved Tanker Structure against Collision and Grounding Damage. Proceedings of the 7th PRADS, 173-179.

Krzysztof W, and Przemyslaw K. 2003 The effect of selected parameters on ship collision results by dynamic FE simulations, Finite Elements in Analysis and Design vol. 39 985–1006

Kuroiwa T. 1996. Numerical simulation of actual collision and grounding experiments. International Conference on Design and Methodologies for Collision and Grounding Protection of Ships, San Francisco.

Mizukami, M., Masayuki, T., Nagahama, S., and Kamei, S. 1996 Collision simulation of a double hulled structure with uni-directional girder system. Proceedings, 6th International Offshore and Polar Engineering Conference, Los Angeles.

Servis, D. and Samuelides, M. 2000 Ship collision analysis using finite elements. IASS-IACM 2000, 4th International Colloquium on Computation of Shell & Spatial Structures. Chania-Greece.

Servis D, Samuelides M, Louka T and Voudouris G. 2002 Implementation of Finite-Element Codes for the Simulation of Ship-Ship Collisions Journal of Ship Research, Vol. 46, No. 4, pp. 239–247

Vredevelde, A. W., Wevers, L. J., and Lemmen, P. P. M. 1993 Full scale collision tests. 3rd International Symposium on Structural Crashworthiness and Failure, Liverpool.

Wu F., Spong R. and Wang G. 2004. Using Numerical Simulation to Analyze Ship Collision. The three International Conference on Collision and Grounding of Ships. Izu, Japan, October 27-33

Zhang L., Egge E. And Bruhns H. 2004 Approval Procedure Concept for Alternative Arrangements The three International Conference on Collision and Grounding of Ships. Izu, Japan, October pp 87-96